European Heart Journal
doi:10.1093/eurheartj/eht344

Coronary evaginations are associated with positive vessel remodelling and are nearly absent following implantation of newer-generation drug-eluting stents: an optical coherence tomography and intravascular ultrasound study

Maria D. Radu[1,2†], Lorenz Räber[1,3†], Bindu Kalesan[4], Takashi Muramatsu[1], Henning Kelbæk[2], Jungho Heo[1], Erik Jørgensen[2], Steffen Helqvist[2], Vasim Farooq[1], Salvatore Brugaletta[1], Hector M. Garcia-Garcia[5], Peter Jüni[4], Kari Saunamäki[2], Stephan Windecker[3], and Patrick W. Serruys[1]*

[1]Thoraxcenter, Erasmus University Medical Centre, Ba583a, 's-Gravendijkwal 230, 3015 CE Rotterdam, Netherlands; [2]Rigshospitalet, Copenhagen University Hospital, Copenhagen, Denmark; [3]Department of Cardiology, Bern University Hospital, Bern, Switzerland; [4]Institute of Social and Preventive Medicine, Bern University, Bern, Switzerland; and [5]Cardialysis BV, Rotterdam, Netherlands

Objectives	The purpose of this study was to assess the occurrence, predictors, and mechanisms of optical coherence tomography (OCT)-detected coronary evaginations following drug-eluting stent (DES) implantation.
Background	Angiographic ectasias and aneurysms in stented segments have been associated with a risk of late stent thrombosis. Using OCT, some stented segments show coronary evaginations reminiscent of ectasias.
Methods	Evaginations were defined as outward bulges in the luminal contour between struts. They were considered major evaginations (MEs) when extending ≥ 3 mm along the vessel length, with a depth $\geq 10\%$ of the stent diameter. A total of 228 patients who had sirolimus (SES)-, paclitaxel-, biolimus-, everolimus (EES)-, or zotarolimus (ZES)-eluting stents implanted in 254 lesions, were analysed after 1, 2, or 5 years; and serial assessment using OCT and intravascular ultrasound (IVUS) was performed post-intervention and after 1 year in 42 patients.
Results	Major evaginations occurred frequently at all time points in SES (~26%) and were rarely seen in EES (3%) and ZES (2%, $P = 0.003$). Sirolimus-eluting stent implantation was the strongest independent predictor of ME [adjusted OR (95% CI) 9.1 (1.1−77.4), $P = 0.008$]. Malapposed and uncovered struts were more common in lesions with vs. without ME (77 vs. 25%, $P < 0.001$ and 95 vs. 20%, $P < 0.001$, respectively) as was thrombus [49 vs. 14%, OR 7.3 (95% CI: 1.7−31.2), $P = 0.007$]. Post-intervention intra-stent dissection and protrusion of the vessel wall into the lumen were associated with an increased risk of evagination at follow-up [OR (95% CI): 2.9 (1.8−4.9), $P < 0.001$ and 3.3 (1.6−6.9), $P = 0.001$, respectively]. In paired IVUS analyses, lesions with ME showed a larger increase in the external elastic membrane area (20% area change) compared with lesions without ME (5% area change, $P < 0.001$).
Conclusion	Optical coherence tomography-detected MEs are a specific morphological footprint of early-generation SES and are nearly absent in newer-generation ZES and EES. Evaginations appear to be related to vessel injury at baseline; are associated with positive vessel remodelling; and correlate with uncoverage, malapposition, and thrombus at follow-up.
Keywords	Optical coherence tomography • Intravascular ultrasound • Coronary evaginations • Early-generation drug-eluting stents • Newer-generation drug-eluting stents • Positive remodelling • Malapposition • Uncovered stent struts

---

† M.D.R. and L.R. contributed equally to this work.

*Corresponding author. Tel: +31 104635260, Fax: +31 104369154, Email: p.w.j.c.serruys@erasmusmc.nl

Introduction

Early-generation drug-eluting stents (DESs) have been associated with an increased risk of very late stent thrombosis (ST) due to delayed arterial healing with evidence of prolonged inflammation, resulting in incomplete endothelialization and acquired malapposition.[1,2] Owing to an ultrahigh resolution (10 μm), optical coherence tomography (OCT) allows an *in vivo* histology-like evaluation of coronary arteries and implanted devices, including the identification of uncovered and malapposed struts.[3,4] Using OCT, it has been observed that some stented segments show outward vessel bulging—'coronary evaginations'—of the luminal contour between struts during the follow-up.[5,6] Three-dimensional (3D) visualization of these segments suggests an ectatic appearance of the vessel wall reminiscent of that seen in angiographic ectasias and aneurysms, which were previously shown to be associated with cardiovascular adverse events.[7,8] Although both drugs and polymers of DES have been suspected as culprits for these changes, the specific mechanisms of the luminal enlargement remain unknown and can only be determined with serial invasive assessment. At present, there are no data on the occurrence, predictors, and mechanisms of OCT-detected coronary evaginations following implantation of early- and newer-generation DES. The objectives of the present study were therefore to assess evaginations using OCT at follow-up in a large cohort of patients; and to investigate the underlying mechanism by serial investigations with OCT and intravascular ultrasound (IVUS) in a subset of patients.
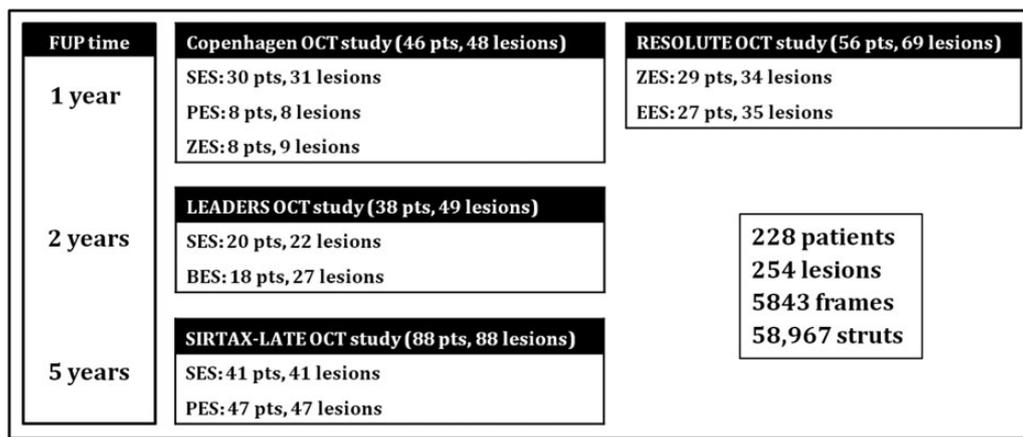
Methods

Study population

The pooled analysis included OCT acquisitions from the LEADERS-, RESOLUTE-, and SIRTAX-LATE OCT substudies, and from the Copenhagen OCT registry, employing the following stents: Cypher Select® (Cordis, Johnson and Johnson, Warren, NJ, USA); Taxus Express® (Boston Scientific, Natick, MA, USA); Endeavor Resolute® (Medtronic, Inc., Santa Rosa, CA, USA); Xience V® (Abbott Vascular, Santa Clara, CA, USA); and Biomatrix® (Biosensors, Inc., Newport Beach, CA, USA).

The design and eligibility criteria for LEADERS-, RESOLUTE-, and SIRTAX-LATE OCT substudies are described in detail elsewhere.[6,9,10] The Copenhagen OCT registry was a single-centre prospective non-randomized evaluation of strut coverage and apposition at 12-month follow-up in relation to apposition at baseline, using the Cypher Select®, Taxus Express®, and Endeavor Resolute® stents. Patients were eligible if they had ≥1 lesion with >50% diameter stenosis in a native coronary artery, with a reference vessel diameter between 2.25 and 4.0 mm. Exclusion criteria were ST-segment elevation myocardial infarction (MI), left ventricular ejection fraction <30%, renal insufficiency (creatinine >133 μmol/L), and lesion location in the left main stem or bypass graft. Optical coherence tomography and IVUS were performed after a satisfactory angiographic result, defined as a residual diameter stenosis <20% and thrombus in MI flow grade 3, and imaging with both modalities was repeated at 1-year follow-up. A total of 56 consecutive patients were included at baseline out of which eight withdrew consent for follow-up, and two were excluded due to system failure or insufficient quality for analysis. *Figure 1* shows an overview of the number of patients, lesions, and stent types included in each cohort, and the time point of OCT acquisition.

Out of the 46 patients with 48 lesions from the Copenhagen OCT registry, 43 patients with 45 lesions were available with complete serial OCT assessment at baseline and follow-up. Out of these, 40 patients with 42 lesions had a serial IVUS assessment. All studies were conducted in accordance with the Declaration of Helsinki and approved by the ethical committees of the involved centres. All patients provided written informed consent prior to the enrolment.

Optical coherence tomography and intravascular ultrasound acquisitions

Optical coherence tomography-images were acquired with commercially available time-domain M2 and M3 systems; and the frequency-domain C7 system from LightLab/St Jude (Westford, MA, USA) at a frame rate of 15.6, 20, and 100 frames/s; and a pullback speed of 1, 3, and 10 mm/s; with the M2, M3, and C7, respectively. Acquisition with occlusive (M2) and non-occlusive (M3 and C7) techniques was described previously.[11] Intravascular ultrasound images were acquired with the Atlantis SR Pro 40 MHz catheter and iLab system (Boston Scientific, Natick, MA, USA) at a frame rate of 30 frames/s and pullback speed of 0.5 mm/s, according

| FUP time		
1 year	**Copenhagen OCT study (46 pts, 48 lesions)** SES: 30 pts, 31 lesions PES: 8 pts, 8 lesions ZES: 8 pts, 9 lesions	**RESOLUTE OCT study (56 pts, 69 lesions)** ZES: 29 pts, 34 lesions EES: 27 pts, 35 lesions
2 years	**LEADERS OCT study (38 pts, 49 lesions)** SES: 20 pts, 22 lesions BES: 18 pts, 27 lesions	**228 patients 254 lesions 5843 frames 58,967 struts**
5 years	**SIRTAX-LATE OCT study (88 pts, 88 lesions)** SES: 41 pts, 41 lesions PES: 47 pts, 47 lesions	

Figure 1 Overview of the optical coherence tomography data used for the pooled analysis. FUP, follow-up; SES, sirolimus-eluting stent; PES, paclitaxel-eluting stent; ZES, zotarolimus-eluting stent; EES, everolimus-eluting stent; BES, biolimus-eluting stent.

to accepted standards. As for serial investigations, the same imaging systems were used at baseline and follow-up.

Optical coherence tomography image analysis

The region of interest included the stented segments which were analysed systematically at 1 mm intervals according to corelab standards (Cardialysis, BV, Rotterdam, The Netherlands). The methodology is shown in *Figure 2A*. The lumen- and stent area were assessed as previously reported.[12] *Malapposition* was considered to be present when the distance from the endoluminal strut border to the lumen contour was larger than the sum of strut metal + polymer thickness, resulting in cut-offs of $\geq$160 μm for Cypher, $\geq$160 μm for Taxus Express, $\geq$100 μm for Endeavor Resolute, $\geq$90 μm for Xience V, and $\geq$130 μm for the Biomatrix stent.[10,12,13] In case of malapposition, the incomplete
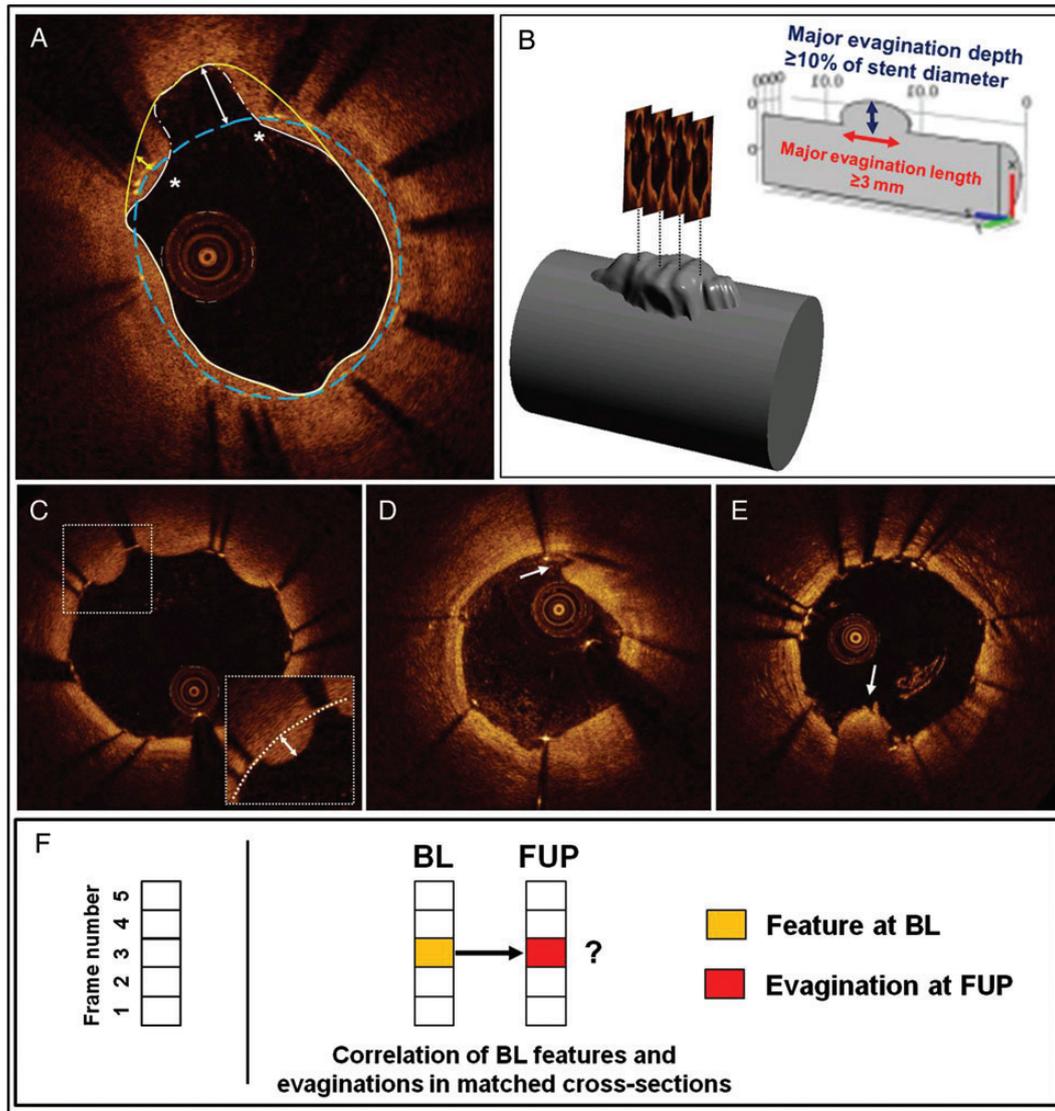
Figure 2 Overview of optical coherence tomography image analysis. (*A*) Frame-level analysis included the assessment of the stent area (blue-broken trace) and lumen area (white trace). Evaginations were defined as bulges in the luminal contour between struts with a maximum depth (white double-headed arrow) exceeding the actual strut thickness. Evagination areas were delineated by the stent contour towards the centre of the lumen and the lumen contour in the opposite direction (broken trace along the luminal contour at 11 o'clock). Struts projecting into the lumen without separation from the vessel wall were defined as protruding when the distance (yellow double-headed arrow) from the stent area trace to a 'lumen help line' (yellow trace extrapolated between deepest point of evaginations and lumen contour) exceeded the actual strut thickness. (*B*) A three-dimensional reconstruction of an evagination. Evaginations were considered major when extending $\geq$3 mm longitudinally, with a depth $\geq$10% of the stent diameter. Prolapse (*C*) was defined as convex-shaped tissue projecting into the lumen between struts without disruption of the luminal continuity, and registered only when the distance from the stent area trace (white-dotted line) to the maximum point of prolapse was $\geq$150 μm. Intra-stent dissections (*D*) were defined as disruptions of the luminal vessel contour within the stented segment, whereas tissue protrusion (*E*) was defined as a mass with an irregular surface attached to the vessel wall or struts and protruding into the lumen. Various features at baseline (i.e. prolapse, intra-stent dissection, tissue protrusion, and malapposed struts) were cross-correlated with the presence of evaginations in matched cross-sections at follow-up (*F*).

stent apposition (ISA) area was measured. Struts projecting into the lumen without obvious separation from the vessel wall were labelled *protruding* when the distance from the strut marker to a 'lumen help line' exceeded that of the actual strut thickness, using the same cut-offs as for malapposition.[5,6] The 'lumen help line' was drawn by extrapolating a trace line between the deepest points in evagination/s and the luminal vessel contour laterally. Struts within overlapped segments and those overlying side branch ostia were excluded from the analysis. Struts were considered *uncovered* if any part of the strut was visibly exposed to the lumen, and covered if a layer of tissue was identified above the struts.[3]

A *coronary evagination* (*Figure 2A*) was defined as the presence of an outward bulge in the luminal vessel contour between apposed struts with a maximum *depth* of the bulge exceeding that of the actual strut thickness, as measured semi-automatically from the deepest point in the bulge to the stent area trace using the thickness-ruler function.[6] The same cut-offs as for malapposition were used. For each evagination, we assessed the *evagination area* defined as the area limited by the stent contour towards the centre of the lumen and the lumen

contour in the opposite direction. Imaging of evaginations with both time- and Fourier-domain OCT systems was performed in a few cases, excluding any influence of OCT system on the appearance of evaginations.

Evaginations may extend over several consecutive cross-sections, giving the vessel an ectatic appearance by 3D reconstruction (*Figure 2B*). Thus, evaginations can be characterized both at the 2D cross-sectional level, and along the length of the stented segment. We assessed the presence of *major evagination* (ME), defined as the occurrence of cross-sectional evagination in ≥3 adjacent frames (i.e. minimum 3 mm of length) with a minimal evagination depth of 10% of the nominal stent diameter. Evagination areas of the various cross-sections belonging to a ME were assumed to be constant 0.5 mm proximal and distal to the analysed cross-section in order to calculate evagination volumes for each 1 mm segment. If evaginations were present in adjacent cross-sections, they were assumed to be in a continuum, and their volumes were summed up to calculate the total *evagination volume*. In addition, we assessed the presence of thrombus defined as a mass ≥100 μm in diameter with an irregular surface attached to the vessel wall or struts and protruding into the lumen.

Table 1 Baseline demographics and baseline patient and lesion level predictors of major evaginations adjusted for time to follow-up

Characteristics	Entire cohort	Major evagination at follow-up		Crude OR (95% CI)	P-value	Adj OR (95% CI)	P-value
	n (%)	Yes, n (%)	No, n (%)				
No. of patients	228	31	197				
Age	60.0 ± 10.4	59.2 ± 11.0	60.2 ± 10.3	1.00 (0.96−1.04)	1.00	1.00 (0.96−1.05)	0.89
Male gender	179 (78.5)	24 (77.2)	155 (78.7)	0.88 (0.35−2.26)	0.78	0.89 (0.33−2.41)	0.82
Hypertension	127 (55.7)	15 (48.4)	112 (56.9)	0.77 (0.35−1.69)	0.52		
Hyperlipidaemia	153 (67.1)	20 (64.5)	133 (67.5)	0.87 (0.38−2.00)	0.74		
Diabetes mellitus	44 (19.3)	4 (12.9)	40 (20.3)	0.58 (0.19−1.80)	0.35		
Current/previous smoker	87 (38.2)	11 (35.5)	76 (38.6)	0.75 (0.33−1.71)	0.49		
Previous MI	58 (25.7)	6 (19.4)	52 (26.7)	0.68 (0.26−1.82)	0.45		
LVEF ≤50	42 (18.4)	12 (38.7)	30 (15.2)	3.20 (1.32−7.72)	0.01	2.71 (1.03−7.16)	0.044
STEMI	48 (21.1)	9 (29.0)	39 (19.8)	1.89 (0.74−4.82)	0.19	1.48 (0.49−4.44)	0.48
Stent type					0.0055		0.0084
EES (reference)	27 (11.8)	1 (3.2)	26 (13.2)	Reference		Reference	
PES	55 (24.1)	4 (12.9)	51 (25.9)	2.06 (0.19−22.48)		1.96 (0.17−22.53)	
BES	18 (7.9)	2 (6.5)	16 (8.1)	3.26 (0.27−39.38)		3.80 (0.31−46.61)	
ZES	37 (16.2)	1 (3.2)	36 (18.3)	0.72 (0.04−12.08)		0.83 (0.05−14.01)	
SES	91 (40.0)	23 (74.2)	68 (34.5)	8.84 (1.07−72.97)		9.05 (1.06−77.35)	
Multivessel disease	23 (13.4)	3 (10.3)	20 (14.0)	0.61 (0.15−2.57)	0.51		
No. of lesions	254	33	221				
Target vessel					0.15		
Left main (reference)	3 (1.2)	1 (3.1)	2 (0.9)	Reference			
LAD	101 (40.0)	7 (21.9)	94 (43.1)	0.16 (0.01−2.45)	0.19		
Circumflex	57 (22.8)	7 (21.9)	50 (22.9)	0.20 (0.01−3.26)	0.26		
RCA	88 (35.2)	17 (53.1)	71 (32.6)	0.47 (0.03−6.93)	0.58		
Graft	1 (0.4)	0 (0)	1 (0.5)	0.16 (0.01−2.45)	0.19		
Stent diameter[a]	3.0 ± 0.4	3.1 ± 0.4	3.0 ± 0.4	7.05 (0.42−119.3)	0.18		
Total stented length[a]	21.6 ± 13.9	22.6 ± 10.4	21.4 ± 14.3	1.00 (0.91−1.11)	0.96		
Stents per lesion[a]	1.4 ± 0.7	1.4 ± 0.8	1.4 ± 0.7	0.91 (0.07−11.12)	0.94		

[a]Expressed as means ± SD.

The Copenhagen OCT registry included OCT examinations at baseline and 1-year follow-up. Cross-sections at baseline and follow-up were matched on the basis of distance from stent borders and the presence of anatomical landmarks such as side branches. This allowed the following serial assessments at the cross-sectional level (*Figure 2C−E*):

At baseline, we assessed the presence of tissue prolapse, intra-stent dissection and tissue protrusion. *Tissue prolapse* was defined as convex-shaped tissue with a regular surface protruding into the lumen between adjacent struts without disruption of the continuity of the luminal vessel surface.[14] The tissue was considered prolapsing only when the distance from the stent area trace to the maximum point of prolapse was ≥ 150 μm, chosen arbitrarily since some degree of prolapse can be seen in most cross-sections. *Intra-stent dissections* were defined as disruptions of the luminal vessel contour within the stented segment, whereas *tissue protrusion* was defined as a mass with an irregular surface attached to the vessel wall or struts and protruding into the lumen. These features as well as the presence of ≥ 1 malapposed strut were then correlated with the presence of evagination at the time of serial follow-up, in matched cross-sections (*Figure 2F*).

Intravascular ultrasound image analysis

Intravascular ultrasound pullbacks were analysed off-line using the QCU-CMS software (Medis, Leiden, The Netherlands) at standard 1 mm intervals, in the same region of interest as for OCT, following the international consensus.[15] Accordingly, we measured the lumen-, stent-, and external elastic membrane area, the latter referred to as vessel area. The plaque and media (P&M) area was calculated as (vessel area − stent area − lumen area outside the stent), and the plaque burden as (P&M area/vessel area) × 100. Positive vessel remodelling was defined as an increase in the vessel area from baseline to follow-up.

Statistical analysis

We used Bayesian hierarchical random-effects model based on Markov chain Monte−Carlo simulation methods[16] with non-informative priors, to compare OCT features such as strut malapposition, protrusion, and coverage between lesions with ME and lesions without. The model included random-effects at the level of cross-sections and lesions, accounting for the correlation of characteristics of cross-sections within lesions, and assigning analytical weights to each lesion depending on the number of struts or cross-sections observed per lesion. Continuous characteristics of lesions such as lumen area and stent area were compared between lesions with vs. without ME using frequentist mixed maximum-likelihood regression models with study cohort, type of stent, patient, and/or lesion as random intercepts. Means and standard deviations were estimated from predicted values. To determine the association of characteristics of lesions and patients at baseline with the presence or absence of ME at follow-up, we used mixed maximum logistic regression models adjusted for time to follow-up (1, 2, or 5 years) with study cohort, type of stent and lesion specified as random intercepts. The same model was used to analyse stent and lumen area over time as assessed with OCT and IVUS in the Copenhagen OCT registry. Mixed maximum logistic regression models with type of stent, patient, and lesion as random intercepts were used to assess the association of the baseline cross-sectional OCT features intra-stent dissection, strut malapposition, tissue protrusion, and prolapse with cross-sectional evagination at follow-up, with univariable and multivariable mutual adjustments for all four features. Statistical analyses were performed using WinBUGS version 1.4.3 (Imperial College and MRC, UK) and Stata, version 11.0 (StataCorp, College Station, TX, USA).

Results

Incidence and extent of evaginations

A total of 228 patients with 254 lesions containing 5843 frames with 58 967 struts were included in the analysis (*Figure 1*). Overall, 75.8% of patients were male and 19.3% had diabetes (*Table 1*). The clinical setting at stent implantation was STEMI in 21.1% of cases, and 40.0% of patients received a SES. Overall, a median (IQR) of 19 (15−26) cross-sections and 183 (140−273) struts were analysed per lesion. Out of 254 lesions, 152 (59.8%) had at least one cross-section with evagination, and 33 (13.0%) lesions contained at least one ME. Out of the 33 lesions with ME, 23 had a SES implanted, four a PES, four a BES, one a ZES, and one an EES. The frequency of cross-sectional and ME according to stent type and time point of implantation are shown in *Table 2*. Both 'any' cross-sectional and ME were more frequent in the SES group when compared with the PES-, ZES-, and EES-groups. The frequency of ME was low for lesions treated with ZES and EES at 1 year, and PES at 5 years.

Table 3 shows the mean evagination- and ISA volumes per lesion in lesions with any cross-sectional evagination and lesions with ME according to stent type and time since implantation. Evagination volumes were consistently larger for the SES group when compared with the other stents. Incomplete stent apposition volumes were similarly larger in SES at 2 and 5 years. Evaluating SES alone, there was a trend for an increase in ISA volumes from 1 to 2 to 5 years (all lesions: $P = 0.024$; lesions with any cross-sectional evagination:

Table 2 Occurrence of cross-sectional and major evaginations stratified by stent type and time to follow-up

Lesions	SES	PES	BES	ZES	EES	*P*-value
No. of lesions with any evagination/total no. of lesions (%)						
Year 1	22 /31 (71)	4 /8 (50)		25 /43 (58)	13 /35 (37)	0.045
Year 2	16/22 (73)		15 /27 (56)			0.25
Year 5	29 /41 (71)	28/47 (60)				0.37
No. of lesions with major evagination/total no. of lesions (%)						
Year 1	8/31 (26)	1 /8 (13)		1 /43 (2)	1 /35 (3)	0.003
Year 2	4/22 (18)		4 /27 (15)			1.00
Year 5	11/41 (27)	3/47 (6)				0.02

Table 3 Evagination and incomplete stent apposition volumes at the lesion level in lesion with any and major evaginations by stent type and time to follow-up

	SES	PES	BES	ZES	EES	*P*-value
At Year 1						
Lesions with any evagination						
EV	2.24 ± 1.68 (22)	0.50 ± 0.72 (4)		0.38 ± 1.79 (25)	0.42 ± 1.29 (13)	0.002
ISAV	0.20 ± 2.12 (22)	3.00 ± 0.90 (4)		0.76 ± 2.25 (25)	2.20 ± 1.63 (13)	0.30
Lesions with ME						
EV	24.20 ± 1.77 (8)	5.31 ± 0.59 (1)		4.42 ± 0.59 (1)	10.28 ± 0.59 (1)	0.39
ISAV	0.54 ± 1.64 (8)	12.10 ± 0.58 (1)		0.26 ± 0.58 (1)	6.23 ± 0.58 (1)	<0.001
All lesions						
ISAV	0.14 ± 1.80 (31)	1.51 ± 0.92 (8)		0.57 ± 2.12 (43)	0.92 ± 1.92 (35)	0.17
At Year 2						
Lesions with any evagination						
EV	2.47 ± 2.52 (16)		0.57 ± 2.44 (15)			0.03
ISAV	1.54 ± 3.32 (16)		0.19 ± 3.21 (15)			0.24
Lesions with ME						
EV	30.40 ± 1.30 (4)		4.08 ± 1.19 (4)			0.01
ISAV	5.22 ± 5.15 (4)		0.79 ± 5.15 (4)			0.21
All lesions						
ISAV	1.34 ± 2.69 (22)		0.12 ± 2.98 (27)			0.12
At Year 5						
Lesions with any evagination						
EV	2.54 ± 1.58 (29)	0.72 ± 1.55 (28)				<0.001
ISAV	3.81 ± 6.69 (29)	1.42 ± 6.57 (28)				0.10
Lesions with ME						
EV	11.80 ± 0.59 (11)	4.40 ± 0.25 (3)				0.008
ISAV	7.47 ± 13.52 (11)	1.91 ± 7.06 (3)				0.41
All lesions						
ISAV	2.72 ± 5.49 (41)	1.04 ± 5.88 (47)				0.09

ME, major evagination; EV, evagination volume; ISAV, incomplete stent apposition volume. Volumes are expressed as means ± SD (no. of lesions) mm^3 and predicted from maximum-likelihood models.

P = 0.016; lesions with ME: *P* = 0.14). The average depths and lengths of cross-sectional and ME are presented in the appendix.

Predictors of major evaginations

Table 1 presents patient and lesion characteristics and their association with ME. The indication for stent implantation was STEMI in 29.0% of patients with and 19.8% of patients without ME (*P* = 0.19). Left ventricular ejection fraction ≤50% was more frequent in patients with compared with those without ME, and the use of SES emerged as an independent predictor for the presence of ME.

Pooled optical coherence tomography analysis

The quantitative results of the OCT analysis at the time of follow-up are shown in *Table 4*. Minimal and average lumen and stent areas were larger in lesions with when compared with those without ME.

Malapposed, protruding, and uncovered struts were more common in lesions with than without ME, and found in 77.2 vs. 24.9% (*P* < 0.001), 97.0 vs. 82.1% (*P* < 0.001), and 94.6 vs. 20.1% (*P* < 0.001) lesions, respectively. Similarly, the proportion of lesions with ≥10% malapposed and uncovered struts was significantly larger in the ME group. The average (means ± SD) thickness of strut coverage was smaller in lesions with MEs compared with those without this feature [0.11 ± 0.29 vs. 0.14 ± 0.23 mm; difference (95% CI): −0.03 (−0.06 to −0.004) mm, *P* = 0.022]. At follow-up, thrombus was more frequent in lesions with 'any' evagination [28.0 vs. 5.9%, OR (95% CI): 6.1 (2.0–17.1), *P* = 0.001] as well as ME [48.5 vs. 14.0%, OR (95% CI): 7.3 (1.7–31.5), *P* = 0.007].

Serial optical coherence tomography and intravascular ultrasound analyses

Quantitative serial OCT results are shown in *Table 5*. All lesions with ME were implanted with SES. The stent and lumen areas were larger

Table 4 Results of follow-up optical coherence tomography analysis

	Major evagination at follow-up		Difference (95% CI)	*P*-value
	Yes	No		
Lesions analysed, *n*	33	221		
Frames analysed, *n*	804	5039		
Struts analysed, *n*	8385	50,582		
Lumen area, mm^{2a}	8.34 ± 5.90	6.44 ± 2.50	1.90 (1.08−2.72)	<0.001
Minimal lumen area, mm^{2a}	5.99 ± 5.60	4.88 ± 2.20	1.12 (0.34−1.89)	0.005
Stent area, mm^{2a}	8.50 ± 6.10	7.37 ± 3.00	1.13 (0.33−1.93)	0.006
Minimal stent area, mm^{2a}	6.71 ± 6.40	5.88 ± 3.70	0.83 (0.03−1.62)	0.04
Strut type, % (95% CrI)				
Malapposed struts[b]				
Malapposed struts per lesion	1.07 (0.41−2.62)	0.11 (0.06−0.17)	0.96 (0.31−2.52)	<0.001
Lesions with ≥1	77.20 (52.80−92.80)	24.9 (15.40−34.90)	51.80 (25.40−72.60)	<0.001
Lesions with ≥10%	5.53 (0.86−19.30)	0.18 (0.02−1.19)	5.24 (0.70−18.90)	0.001
Protruding struts[b]				
Protruding struts per lesion	3.04 (1.52−5.87)	0.11 (0.06−0.17)	2.92 (1.42−5.77)	<0.001
Lesions with ≥1	97.00 (86.70−99.60)	82.1 (72.30−89.60)	14.30 (4.04−23.80)	0.01
Lesions with ≥10%	9.34 (2.03−27.10)	4.93 (1.93−10.80)	4.09 (-3.42−21.20)	0.37
Uncovered struts[b]				
Uncovered struts per lesion	3.82 (2.12−6.82)	1.39 (1.06−1.79)	2.43 (0.70−5.46)	0.002
Lesions with ≥1	94.60 (81.00−99.10)	20.10 (11.40−30.00)	74.00 (56.00−85.80)	<0.001
Lesions with ≥10%	5.59 (0.85−19.30)	<0.01 (<0.01−0.16)	5.57 (0.84−19.30)	<0.001

Lumen and stent areas are expressed as means ± SD.
CrI, credibility interval.
[a]Using traditional mixed maximum-likelihood model.
[b]Using Bayesian hierarchical 2-level logistic regression model.

Table 5 Quantitative serial optical coherence tomography results of the stented segment

	Major evagination at follow-up		Difference (95% CI)	*P*-value
	Yes	No		
Patients analysed, *n*	8	35		
Lesions analysed, *n*	8	37		
Frames analysed, *n*	154	705		
SA BL, mm^2	8.60 ± 1.42	7.14 ± 1.22	1.84 (0.32−3.37)	0.02
SA FUP, mm^2	9.21 ± 1.59	7.33 ± 1.36	2.28 (0.57−3.98)	0.009
SA change, mm^2	0.61 ± 0.29	0.20 ± 0.24	0.43 (-0.02−0.88)	0.06
LA BL, mm^2	8.85 ± 1.11	7.30 ± 0.92	1.89 (0.45−3.33)	0.01
LA FUP, mm^2	9.03 ± 1.22	6.29 ± 1.01	2.89 (1.27−4.52)	<0.001
LA change, mm^2	0.17 ± 0.66	−1.00 ± 0.59	0.99 (0.29−1.69)	0.006

Areas are presented as means ± SD.
SA, stent area; LA, lumen area; BL, baseline; FUP, follow-up.

in lesions with when compared with those without ME at both baseline and follow-up, with a significant change in the lumen area at follow-up in both groups [increase in the lumen area in lesions with ME (*P* = 0.01), and decrease in the lumen area in lesions without ME (*P* < 0.001)]. The change in the stent area from baseline to follow-up within the ME group was not significant (*P* = 0.15).

Table 6 shows the association of OCT characteristics recorded at baseline with cross-sectional evagination at follow-up in matched

Table 6 Assessment of the correlation of baseline optical coherence tomography features and evaginations, in matched cross-sections

	Evagination at follow-up		Crude OR (95% CI)	*P*-value	Multivariable OR (95% CI)	*P*-value
	Yes	**No**				
No. of frames at follow-up	128	713				
Characteristics of cross-section at baseline						
Intra-stent dissection, *n* (%)	60 (46.9)	159 (21.8)	3.01 (1.81–5.00)	<0.001	2.93 (1.75–4.89)	<0.001
Malapposed strut, *n* (%)	12 (9.4)	35 (4.8)	1.76 (0.77–4.03)	0.18	1.69 (0.72–3.99)	0.23
Tissue protrusions, *n* (%)	27 (21.1)	73 (10.0)	3.27 (1.59–6.70)	0.001	3.34 (1.61–6.93)	0.001
Prolapse, *n* (%)	26 (20.3)	162 (22.2)	1.04 (0.57–1.90)	0.90	1.06 (0.57–1.99)	0.85

Using mixed logistic regression with stent type, patient, and lesion as random intercept.

cross-sections. In both uni- and multivariable analyses, intra-stent dissections, and tissue protrusions at baseline were associated with cross-sectional evagination at follow-up: the odds of evagination at follow-up were increased by about three in the presence of either dissection or tissue protrusion at baseline.

The corresponding serial IVUS analyses are summarized in *Table 7*. At baseline, the vessel area was larger among lesions with ME. Serial IVUS analysis showed a larger increase in the vessel area and positive remodelling in lesions with ME when compared with those without (21.1 vs. 4.6%, *P* < 0.001), mainly driven by an increase in the P&M area and accompanied by an increase in the lumen area. Again, the stent area appeared to increase between baseline and follow-up in lesions with ME (*P* = 0.84), but not in lesions without [difference in change between groups (95% CI): 0.43 (0.01–0.85) mm^2, *P* = 0.04].

Discussion

The present study shows that OCT-detected MEs are specifically related to early-generation SES, and much smaller and in general less frequent in newer-generation DES. The mechanism underlying the pathogenesis of ME was suggestively a positive remodelling. Signs of injury documented immediately after stent implantation were associated with an increased risk of evagination at follow-up.

Positive remodelling as a cause of coronary evagination

Coronary artery ectasias and aneurysms following DES implantation have generated great interest owing to their association with ST.[7,8,17] These vessel distensions have often been accompanied by ISA, suggesting positive remodelling as the underlying pathomechanism, since regional vessel remodelling was previously identified as a cause of late acquired stent malapposition (LASM).[7,17,18] In the present study, we took advantage of information obtained by OCT on depth, cross-sectional area, and longitudinal extent, to assess evaginations in three dimensions. The association between positive remodelling and ME suggests that positive remodelling is the mechanism underlying the pathogenesis of evaginations.

We observed that ME in general occurred more frequently and appeared to be larger in SES, suggesting these to be a specific

morphological footprint of these early-generation DES. Conversely, MEs were less frequent in PES compared with SES at 5 years—a difference which is confirmatory of the SIRTAX-LATE OCT study. At 1 year, MEs were less frequent in PES compared with SES but were almost absent in newer-generation ZES and EES. No difference, however, was observed between SES and BES at 2 years—something that needs to be interpreted in light of a relatively low sample size of only 18 SES and 18 BES patients at 2 years of follow-up. (Accordingly, it cannot be excluded that this finding could be due to chance. Nevertheless, assessment of evagination volumes showed that these were significantly larger for SES compared with BES, thus being in line with the findings in the other subgroups, particularly the SES vs. ZES and EES, where the sample size was also relatively low.) In a meta-analysis, Hassan *et al.*[19] reported similar findings in terms of IVUS-detected LASM, which were also accompanied by positive vessel remodelling, with the highest incidence in SES followed by PES, and newer-generation ZES and EES. These similarities, together with the observed association of ME with malapposed, protruding, and uncovered struts, suggest that these features may be part of the same disease entity.

Pre-clinical and human autopsy studies previously demonstrated that the inflammatory response following DES implantation strongly relates to the type of stent: SES typically induces granulomatous inflammation with macrophages, giant cells, lymphocytes, and eosinophils; PES exhibits extensive fibrin deposition and medial smooth muscle cell necrosis; ZES and EES show only low levels of inflammation and fibrin deposition.[1,20–22] In addition, SES has been associated with marked adventitial inflammation and fibrosis—findings associated with positive remodelling.[20,23] These results are in line with observations of aneurysmal vessel dilation, stent malapposition, and generalized eosinophilic vasculitis in a case of late ST in a patient with SES.[24] Similarly, the extent of vascular remodelling predominantly after SES implantation correlated with the number of eosinophils harvested from thrombus aspirates in patients with very late ST,[25] supporting the notion that OCT-detected ME represent a pathological vascular reaction particularly related to this stent.

If evaginations and protruding struts are precursors of ISA, a stretch in the P&M may occur during the vessel expansion before complete detachment from the stent. Interestingly, we observed a trend towards a decrease in the size of ME from 1 and 2 to 5-year

Table 7 Quantitative serial intravascular ultrasound results of the stented segment

	Major evagination at follow-up		Diff (95% CI)	P-value
	Yes	**No**		
SA BL, mm^2	8.67 ± 1.94	7.61 ± 1.62	1.31 (−0.43 to 3.05)	0.14
SA FUP, mm^2	9.18 ± 2.03	7.67 ± 1.68	1.76 (−0.09 to 3.60)	0.06
SA change, mm^2	0.50 ± 0.31	0.06 ± 0.24	0.43 (0.01 to 0.85)	0.04
LA BL, mm^2	8.67 ± 1.92	7.59 ± 1.61	1.33 (−0.39 to 3.06)	0.13
LA FUP, mm^2	9.28 ± 2.00	7.37 ± 1.63	2.10 (0.24 to 3.97)	0.03
LA change, mm^2	0.59 ± 0.40	−0.22 ± 0.33	0.75 (0.22 to 1.28)	0.006
VA BL, mm^2	16.53 ± 2.63	13.78 ± 1.99	3.44 (0.62 to 6.25)	0.02
VA FUP, mm^2	20.06 ± 3.44	14.41 ± 2.76	6.29 (3.00 to 9.59)	<0.001
VA change, mm^2	3.51 ± 1.19	0.63 ± 1.00	2.84 (1.71 to 3.98)	<0.001
P&M area BL, mm^2	7.86 ± 1.79	6.14 ± 1.56	2.11 (0.52 to 3.70)	0.009
P&M area FUP, mm^2	10.78 ± 2.36	7.02 ± 2.06	4.17 (2.08 to 6.27)	<0.001
P&M area change, mm^2	2.89 ± 0.92	0.87 ± 0.76	2.06 (1.11 to 3.00)	<0.001
PB BL, %	46.82 ± 4.02	44.36 ± 2.95	3.02 (−2.65 to 8.70)	0.30
PB FUP, %	52.78 ± 4.36	48.46 ± 3.15	5.26 (−0.93 to 11.46)	0.10
PB change, %	5.90 ± 1.98	3.95 ± 1.72	2.21 (−0.08 to 4.49)	0.06

Areas are presented as means ± SD.
SA, stent area; LA, lumen area; VA, vessel area; P&M, plaque and media; PB, plaque burden; BL, baseline; FUP, follow-up.

follow-up among SES-stented segments, while there was a trend towards an increase in ISA volume, suggesting that evaginations may transition into ISA. Regarding the large ISA volumes at 1 year in the two cases of PES and ZES with ME; the ISA in the PES represented persistent malapposition, whereas the ISA in ZES was located in the proximity of a large bifurcation and thus likely present at baseline.

The unexpected finding of a larger stent area only in lesions with ME, which was consistent across the pooled analysis as well as the serial independent evaluation with OCT and IVUS, may either be related to the vessel expansion before detachment or due to chance. It is unlikely that a more intense use of nitroglycerine or potentially higher flush rate during OCT acquisition at follow-up when compared with baseline could have induced these findings only in lesions with ME.

Mechanisms of vessel remodelling

The SES-specific remodelling pattern may be triggered by the polymer rather than the drug. Evidence in favour of this hypothesis is the presence of a focal giant cell reaction surrounding polymer remnants separated from the stent struts,[24] together with observations that durable-polymer SES when compared with polymer-free SES and bare-metal stents are associated with a larger external elastic membrane area.[23] Considering that 80% of sirolimus is released from durable-polymer SES within the first 4 weeks, it seems unlikely that sirolimus itself induces long-term alterations of the vessel wall such as the ME detected up to 5 years in the present study.

The specific mechanisms by which polymers may induce positive remodelling in cases of coronary aneurysms and LASM remain speculative. In relation to SES, it is known that methacrylate may exert a toxic effect on endothelial cells and leucocytes, and can modulate pro-coagulant activities of monocytes.[26] Exposure to the poly-n-butyl-methacrylate polymer can furthermore cause delayed (type IV) hypersensitivity reactions mediated at least in part by accumulated CD4 T-helper cells secreting interleukin (IL)-4 and IL-13.[24] Of note, IL-13 was associated with increased smooth muscle cell contractility in asthma,[27] and can induce alveolar remodelling and emphysema in mice via induction of matrix metalloproteinase (MMP)-9 and MMP-12.[28] Both these MMPs were identified as important factors in the development of abdominal aortic aneurysms in humans by degradation of elastin.[29] At the same time, MMP-12 has been found to be a mediator of the accumulation of macrophages and eosinophils.[28] Similar pathways may be responsible for the remodelling and eosinophilia observed in SES-treated coronary arteries. However, then remains the question why not all patients develop this finding.

To further address this, we compared OCT findings following stent implantation with the presence of evaginations at follow-up in corresponding cross-sections. Accordingly, our study demonstrated that cross-sections exhibiting intra-stent dissections and tissue protrusions at baseline—both representing markers of injury—were associated with an increased risk of evagination at the time of OCT follow-up. (Of note, tissue protrusions were defined as tissue projections with irregular lumen contour and thereby suggestive of either thrombus or tissue disruptions other than intra-stent dissections, whereas tissue prolapses were characterized by an intact lumen contour, suggestive of prolapsing plaque.) This relationship is supported by previous observations relating OCT-detected evaginations and coronary artery aneurysms with vessel wall dissections and deep arterial injury caused by oversized balloons, stents, and atherectomy.[5,30,31] Nevertheless, considering that intra-stent
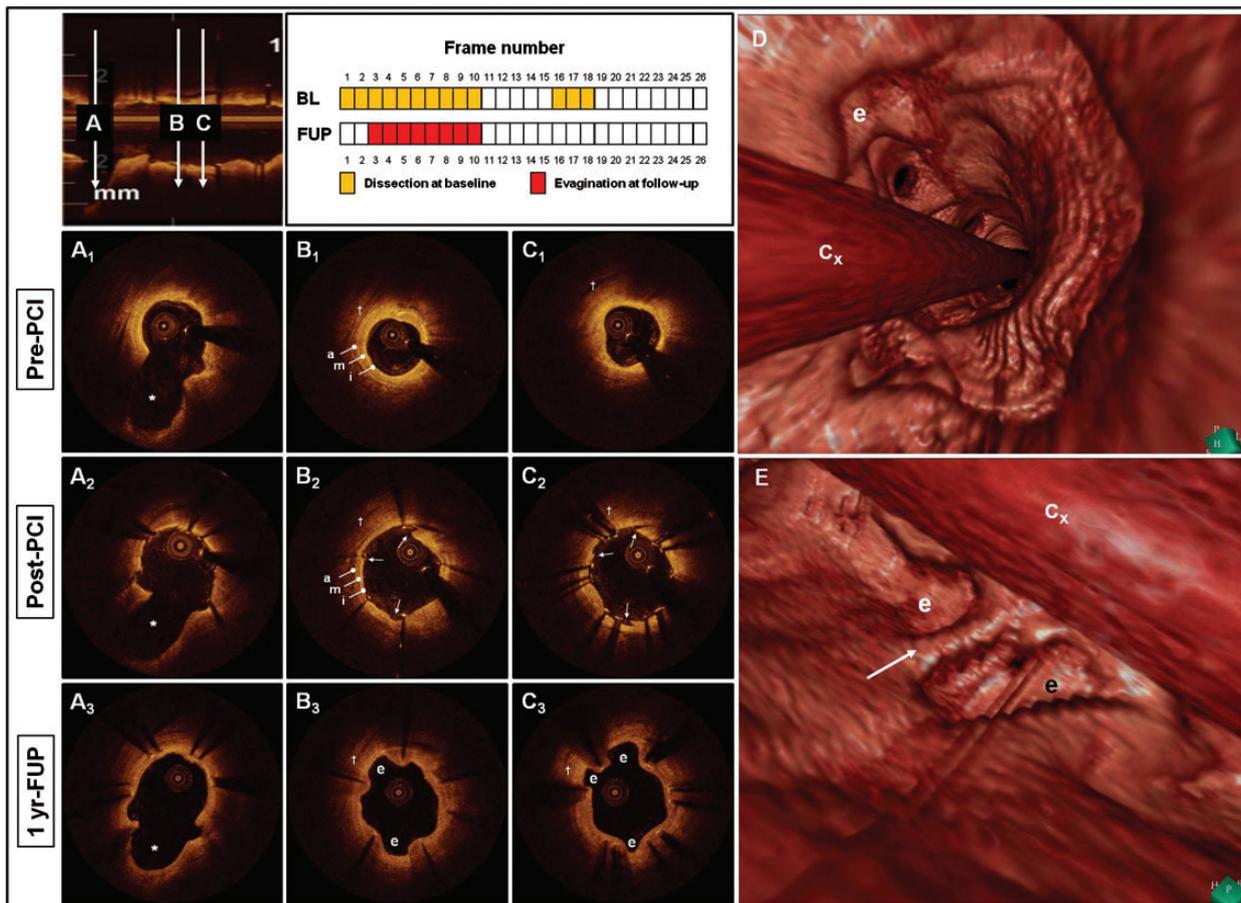
Figure 3 Co-location of intra-stent dissections post-PCI and evaginations at follow-up. ($A–C$) Three cross-sections obtained at corresponding sites before ($A_1–C_1$), immediately after ($A_2–C_2$), and at 1 year ($A_3–C_3$) following stent implantation. The large side-branch (*) in (A_1)–(A_3) confirms a good matching, as does the pericardial space (†) and evidence of trilaminar vessel structure (i, intima; m, media; a, adventitia) in (B_1)–(B_3) and (C_1)–(C_3). In (B_2) and (C_2), a large intra-stent dissection extends from 10 to 1 o'clock (white arrows), exposing the underlying adventitia, and a small dissection is seen at 6 o'clock (white arrow). Of note, evaginations (e) are clearly seen at the corresponding sites at follow-up in (B_3) and (C_3). The upper middle panel shows a schematic overview of the location of intra-stent dissection at baseline and evagination at follow-up within matched frames. (D) An endoscopic three-dimensional view of the vessel in question, where evaginations (e) create an irregular luminal surface. The optical coherence tomography-catheter (Cx) is located to the left of the 'point of view'. (E) A perpendicular view of the evagination in (B_3) and (C_3) at 10 o'clock (white e in (E)), which in the three-dimensional reconstruction is separated from another evagination (black e in (E)) along the vessel segment by a strut (white arrow). The evagination at 12 o'clock in (C_3) is hidden behind the optical coherence tomography-catheter (Cx) in (E).

dissections were present in 27%, 15%, and 31% of cross-sections in SES, PES and ZES, respectively, it may be argued that the influence of stent type, as compared to that of vessel injury, is relatively greater on the development of ME, which in the serially studied lesions were all present in segments implanted with SES. Although the depth of intra-stent dissections could not be systematically assessed due to the limited tissue penetration of OCT, we did observe 12 cases of evaginations following intra-stent dissections extending into the media and adventitia (*Figure 3*).

Potential clinical relevance of coronary evaginations

Features associated with very late ST include uncovered struts, late malapposition, positive remodelling, chronic inflammation as well as ectasias and aneurysms.[1,2,7,8,17,25,32] We found nearly all these features to be more common in lesions with ME, suggesting that ME may be part of the same pathophysiological entity commonly recognized as inappropriate healing following DES implantation, proposing a possible link with late ST. Moreover, our finding of a greater frequency of thrombus in lesions with 'any' and MEs may be an expression of a potential thrombogenicity of these lesions compared with those without evaginations. Although our pooled study sample included one of the largest OCT cohorts to date, it was too small for a meaningful evaluation of such a relationship, however, two of the patients with ME from the SIRTAX-LATE cohort experienced very late ST at 5 and 12 months following 5-year OCT follow-up. Both of these occurred in SES which had some of the most extensive evagination- and ISA volumes in the entire cohort.[6] Along the same line, Alfonso *et al.*[7] described that among patients with angiographic

coronary artery aneurysms, subsequent ST correlated with a larger vessel and lumen volume by IVUS at the time of imaging. Similarly, Imai et al.[8] observed an increased risk of ST and target lesion revascularization in SES with ectasias measuring $\geq 20\%$ of the stent diameter and extending longitudinally at least the length of the stent diameter, corresponding to an ectasia depth and length of 0.6 mm and 3 mm in a 3 mm stent, respectively—a similar length but twice the depth of the ME definition used in our study. These data suggest that the extent of evagination matters and that clarification of the natural history of evaginations as well as the relationship between the degree of evagination and clinical events merits consideration.

Although first-generation SES are no longer manufactured, they have been implanted in a considerable number of patients worldwide. Recent data from a registry of >12 000 patients, and a meta-analysis including 49 trials, suggest that treatment with newer-generation EES is associated with a lower risk of very late ST when compared with early-generation SES and PES,[33,34] which are additionally associated with a continued risk of very late ST when compared with EES. In this context, it is interesting that the occurrence of evaginations, malapposition, and uncoverage by OCT in the present study, as well as the incidence of IVUS-detected LASM in previous studies,[19] follow a similar pattern. Our findings therefore suggest that evaginations detected with high-resolution OCT may be predictors of late ST particularly in SES, and alongside malapposition and uncoverage provide a possible explanation for differences in late adverse ischaemic events in early- compared with newer-generation DES. Conversely, PES when compared with SES showed fewer ME and only a modest increase when compared with newer-generation DES. Although clinical rates of ST have been comparable between SES and PES, the trigger leading to thrombosis appears to differ[21] in view of substantial differences in the frequency of evaginations. Studies assessing clinical outcomes with OCT and IVUS—particularly with serial imaging—are demanding to perform due to the relatively complex and costly set-ups and the large number of patients required. In view of this, the present study, although relatively small with the 254 imaged lesions, provides important new insights into the utility of OCT for assessing vascular reactions following stent implantation, and suggests that this technology can identify features specific for different stents, which may be useful for improving the prediction of events in the future.

Limitations

The following shortcomings must be considered when interpreting the results of the present study. First, we pooled data from four separate cohorts with different time to follow-up, out of which one came from a non-randomized registry. Efforts were made to adjust for these issues by using frequentist and Bayesian mixed models accounting for the clustered nature of data. Secondly, we did not assess the type of malapposition at follow-up primarily as our focus was on evaginations, and since the relationship between acquired malapposition and positive remodelling has already been shown.[18] Considering that positive remodelling is a common denominator of evaginations and LASM, it seems reasonable to assume that the majority of malapposed struts at follow-up within lesions with ME were late acquired,

particularly since there was no correlation between malapposed struts at baseline and ME at follow-up. Thirdly, we extrapolated cross-sectional evagination areas 0.5 mm proximal and distal to the frame of interest to estimate the volume of ME, which may both over- and underestimate the size. Separate evaluation of cross-sectional and ME does however not affect the results of the relative occurrence and predictors of evaginations. Whether this is also true for the mechanisms is unknown since serial IVUS was only available for one of the cohorts. In this regard, it cannot be discarded that evaginations at 2 and 5 years may be caused by mechanisms other than remodelling as observed at 1 year. Furthermore, OCT cross-sections were analysed at 1 mm intervals, although the highest sampling density with commercially available new-generation OCT is 0.2 mm. This could potentially give inaccurate estimates of the occurrence and size of cross-sectional and ME. Considering that gold-standard histology typically evaluates entire lesions based on three to five cross-sections—remarkably lower compared with the average 19 cross-sections per lesion assessed in our study—we chose to accept this level of accuracy, as well as the potential imprecision in the selection of corresponding cross-sections at baseline and follow-up, which is inevitably present whenever serial evaluations are performed. Also, although care was taken to obtain as accurate measurements of evagination- and ISA-volumes as possible, the inherent risk of multiplication of small measurement errors cannot be excluded. Finally, even though this study is one of the largest OCT studies to date, the small number of lesions with MEs, especially in the ZES and EES groups at 1 year, nonetheless limits the power of the study.

Conclusion

Optical coherence tomography-detected MEs are a specific morphological footprint of early-generation SES and are nearly absent in newer-generation ZES and EES. Optical coherence tomography detected intra-stent dissections and tissue protrusions at baseline are associated with an increased risk of evaginations at follow-up. The mechanism underlying the pathogenesis of ME is suggestively a positive remodelling.

Conflict of interest: Dr. S.W. has received consulting and lecture fees from Abbott, Boston Scientific, Biosensors, Cordis, and Medtronic.

Appendix

Addendum to the methodology and results

Optical coherence tomography and intravascular ultrasound image analysis

The *lumen area (LA)* was measured using the automatic area trace function. *Stent struts* were defined as signal-intense spots with dorsal shadowing and a marker was placed at the endoluminal leading edge of the strut, in the mid-point of its axis. The *stent area (SA)* was measured by connecting the strut markers with a trace line. *Strut apposition* was assessed for each strut by measuring the distance from the strut marker to the lumen contour semi-automatically using the thickness-ruler function.

For the LEADERS and RESOLUTE trials, lumen and stent area measurements, strut apposition, and strut coverage were assessed by corelab analysts (Cardialysis) blinded to stent type and clinical outcomes. The OCT analyses of the SIRTAX-LATE OCT substudy, the Copenhagen OCT registry, and the assessment of evaginations and protruding struts in all studies were performed by two observers. In case of disagreement, a referee was consulted to a final decision. The time-consuming assessment of evaginations in the LEADERS, RESOLUTE, and Copenhagen cohorts were performed un-blinded, as blinding would have implied a detailed assessment of evaginations using the cut-off of the thinnest stent (Xience, 90 µm or Resolute, 100 µm), and thus the assessment of a large number of bulges in the thicker stents which would, following un-blinding, not fulfil the definition of evagination. Assessments of OCT cross-sections at baseline and follow-up were performed independently, without knowledge of the characteristics of matched cross-sections. The same methodology was used throughout all four OCT studies.

Intravascular ultrasound analyses were performed by two observers, and in case of disagreement a referee was consulted to reach a final decision. Baseline IVUS assessment was performed independently of the follow-up evaluation, and without knowledge of the results of the OCT analysis.

Details of the Bayesian approach

The proportions of malapposed, protruding, and uncovered struts per lesion were analysed using a model with Bernoulli distribution, while the proportions of lesions with ≥ 1 and $\geq 10\%$ malapposed, protruding, and uncovered struts were analysed using Bayesian hierarchical random-effects model with logit distribution. Estimates were derived from the median of the posterior distribution of the 50 001 to 150 000 iteration, with the initial 50 000 iterations discarded as 'burn-in'. We derived 95% credibility intervals (95% CrI) from the 2.5th and 97.5th percentiles of the posterior distribution, also calculating two-sided *P*-values from the posterior distribution. 95% CrI and *P*-values from posterior distributions can be interpreted similarly to conventional 95% confidence intervals and *P*-values.

Additional details on the evagination size

The average depths and lengths of cross-sectional and ME are presented in the appendix table 1 and 2.

Appendix table 1 Specification of the volume, depth and number of cross-sections spanned for "any" cross-sectional evaginations, by stent type and time to FUP

	SES	PES	BES	ZES	EES	p
At Year 1						
Lesions with any evagination N	*22*	*4*		*25*	*13*	
EV	2.24 ± 1.68	0.50 ± 0.72		0.38 ± 1.79	0.42 ± 1.29	0.002
Max depth	0.36 ± 0.45	0.33 ± 0.19		0.23 ± 0.48	0.25 ± 0.34	0.005
N CS/lesion*	4.02 (2.90−6.68)	2.56 (2.09−3.67)		3.01 (2.34−4.16)	2.26 (1.94−2.88)	0.46
At Year 2						
Lesions with any evagination N	*16*		*15*			
EV	2.47 ± 2.52		0.57 ± 2.44			0.03
Max depth	0.32 ± 0.63		0.26 ± 0.61			0.15
N CS/lesion*	4.41 (3.57−10.96)		2.32 (1.74−8.49)			0.13
At Year 5						
Lesions with any evagination N	*29*	*28*				
EV	2.54 ± 1.58	0.72 ± 1.55				<0.001
Max depth	0.36 ± 0.80	0.30 ± 0.56				0.13
N CS/lesion*	4.44 (3.99−5.92)	2.25 (1.96−2.73)				<0.001

N CS/lesions refers to the number of CSs per lesion with any evagination. Values are presented as means ± SD unless otherwise specified.
EV, evagination volume; CS, cross-section.
*Expressed as median (IQR). Volumes are expressed in mm^3, and depths in mm.

Appendix table 2 Specification of the volume, depth and number of cross-sections spanned for major evaginations, by stent type and time to FUP

	SES	PES	BES	ZES	EES	p
At Year 1						
Lesions with ME N	8	1		1	1	
EV	24.20 ± 1.77	5.31 ± 0.59		4.42 ± 0.59	10.28 ± 0.59	0.39
Max depth	0.57 ± 0.50	0.58 ± 0.17		0.75 ± 0.17	0.69 ± 0.17	0.90
N CS/lesion*	9.00 (7.00−11.00)	6.00 (6.00−6.00)		13.00 (13.00−13.00)	11.00 (11.00−11.00)	0.39
At Year 2						
Lesions with ME N	4		4			
EV	30.40 ± 1.30		4.08 ± 1.19			0.01
Max depth	0.49 ± 0.59		0.43 ± 0.54			0.54
N CS/lesion*	19.00 (12.00−28.50)		7.50 (5.50−11.50)			0.02
At Year 5						
Lesions with ME N	11	3				
EV	11.80 ± 0.59	4.40 ± 0.25				0.009
Max depth	0.58 ± 0.55	0.40 ± 0.23				0.18
N CS/lesion*	7.00 (6.00−12.00)	4.00 (2.00−7.00)				0.06

N CS/lesions refers to the number of CSs per lesion with any evagination. Values are presented as means ± SD unless otherwise specified.
ME, major evagination; CS, cross-section.
*Expressed as median (IQR). Volumes are expressed in mm^3, and depths in mm.

References

1. Joner M, Finn AV, Farb A, Mont EK, Kolodgie FD, Ladich E, Kutys R, Skorija K, Gold HK, Virmani R. Pathology of drug-eluting stents in humans: delayed healing and late thrombotic risk. *J Am Coll Cardiol* 2006;**48**:193−202.
2. Finn AV, Joner M, Nakazawa G, Kolodgie F, Newell J, John MC, Gold HK, Virmani R. Pathological correlates of late drug-eluting stent thrombosis: strut coverage as a marker of endothelialization. *Circulation* 2007;**115**:2435−2441.
3. Tearney GJ, Regar E, Akasaka T, Adriaenssens T, Barlis P, Bezerra HG, Bouma B, Bruining N, Cho JM, Chowdhary S, Costa MA, de Silva R, Dijkstra J, Di Mario C, Dudeck D, Falk E, Feldman MD, Fitzgerald P, Garcia H, Gonzalo N, Granada JF, Guagliumi G, Holm NR, Honda Y, Ikeno F, Kawasaki M, Kochman J, Koltowski L, Kubo T, Kume T, Kyono H, Lam CC, Lamouche S, Lee DP, Leon MB, Maehara A, Manfrini O, Mintz GS, Mizuno K, Morel MA, Nadkarni S, Okura H, Otake H, Pietrasik A, Prati F, Raber L, Radu MD, Rieber J, Riga M, Rollins A, Rosenberg M, Sirbu V, Serruys PW, Shimada K, Shinke T, Shite J, Siegel E, Sonada S, Suter M, Takarada S, Tanaka A, Terashima M, Troels T, Uemura S, Ughi GJ, van Beusekom HM, van der Steen AF, van Es GA, van Soest G, Virmani R, Waxman S, Weissman NJ, Weisz G. Consensus standards for acquisition, measurement, and reporting of intravascular optical coherence tomography studies: a report from the international working group for intravascular optical coherence tomography standardization and validation. *J Am Coll Cardiol* 2012;**59**:1058−1072.
4. Nakano M, Vorpahl M, Otsuka F, Taniwaki M, Yazdani SK, Finn AV, Ladich ER, Kolodgie FD, Virmani R. Ex vivo assessment of vascular response to coronary stents by optical frequency domain imaging. *JACC Cardiovasc Imaging* 2012;**5**:71−82.
5. Radu M, Jorgensen E, Kelbaek H, Helqvist S, Skovgaard L, Saunamaki K. Optical coherence tomography at follow-up after percutaneous coronary intervention: relationship between procedural dissections, stent strut malapposition and stent healing. *EuroIntervention* 2011;**7**:353−361.
6. Räber L, Baumgartner S, Garcia-Garcia H, Kalesan B, Justiz J, Pilgrim T, Moschovitis A, Meier B, Serruys P, Jüni P, Windecker S. Vascular healing response five years after implantation of first-generation DES. The SIRTAX-LATE optical coherence tomography study. *JACC Cardiovasc Interv.* 2012;**5**:946−57.
7. Alfonso F, Perez-Vizcayno MJ, Ruiz M, Suarez A, Cazares M, Hernandez R, Escaned J, Banuelos C, Jimenez-Quevedo P, Macaya C. Coronary aneurysms after drug-eluting stent implantation: clinical, angiographic, and intravascular ultrasound findings. *J Am Coll Cardiol* 2009;**53**:2053−2060.
8. Imai M, Kadota K, Goto T, Fujii S, Yamamoto H, Fuku Y, Hosogi S, Hirono A, Tanaka H, Tada T, Morimoto T, Shiomi H, Kozuma K, Inoue K, Suzuki N, Kimura T, Mitsudo K. Incidence, risk factors, and clinical sequelae of angiographic peri-stent contrast staining after sirolimus-eluting stent implantation. *Circulation* 2011;**123**:2382−2391.
9. Barlis P, Regar E, Serruys PW, Dimopoulos K, van der Giessen WJ, van Geuns RJ, Ferrante G, Wandel S, Windecker S, van Es GA, Eerdmans P, Juni P, di Mario C. An optical coherence tomography study of a biodegradable vs. durable polymer-coated limus-eluting stent: a LEADERS trial sub-study. *Eur Heart J* 2010;**31**:165−176.
10. Gutierrez-Chico JL, van Geuns RJ, Regar E, van der Giessen WJ, Kelbaek H, Saunamaki K, Escaned J, Gonzalo N, di Mario C, Borgia F, Nuesch E, Garcia-Garcia HM, Silber S, Windecker S, Serruys PW. Tissue coverage of a hydrophilic polymer-coated zotarolimus-eluting stent vs. a fluoropolymer-coated everolimus-eluting stent at 13-month follow-up: an optical coherence tomography substudy from the RESOLUTE All Comers trial. *Eur Heart J* 2011;**32**:2454−2463.
11. Prati F, Cera M, Ramazzotti V, Imola F, Giudice R, Albertucci M. Safety and feasibility of a new non-occlusive technique for facilitated intracoronary optical coherence tomography (OCT) acquisition in various clinical and anatomical scenarios. *EuroIntervention* 2007;**3**:365−370.
12. Gonzalo N, Garcia-Garcia HM, Serruys PW, Commissaris KH, Bezerra H, Gobbens P, Costa M, Regar E. Reproducibility of quantitative optical coherence tomography for stent analysis. *EuroIntervention* 2009;**5**:224−232.
13. Barlis P, Tanigawa J, Di Mario C. Coronary bioabsorbable magnesium stent: 15-month intravascular ultrasound and optical coherence tomography findings. *Eur Heart J* 2007;**28**:2319.
14. Gonzalo N, Serruys PW, Okamura T, Shen ZJ, Onuma Y, Garcia-Garcia HM, Sarno G, Schultz C, van Geuns RJ, Ligthart J, Regar E. Optical coherence tomography assessment of the acute effects of stent implantation on the vessel wall: a systematic quantitative approach. *Heart* 2009;**95**:1913−1919.
15. Mintz GS, Nissen SE, Anderson WD, Bailey SR, Erbel R, Fitzgerald PJ, Pinto FJ, Rosenfield K, Siegel RJ, Tuzcu EM, Yock PG. American College of Cardiology Clinical Expert Consensus Document on Standards for Acquisition, Measurement and Reporting of Intravascular Ultrasound Studies (IVUS). A report of the American College of Cardiology Task Force on Clinical Expert Consensus Documents. *J Am Coll Cardiol* 2001;**37**:1478−1492.
16. Spiegelhalter DJ, Myles JP. *Bayesian Approaches to Clinical Trials and Health Care Evaluation*. Chicester: John Wiley & Sons; 2004.
17. Cook S, Wenaweser P, Togni M, Billinger M, Morger C, Seiler C, Vogel R, Hess O, Meier B, Windecker S. Incomplete stent apposition and very late stent thrombosis after drug-eluting stent implantation. *Circulation* 2007;**115**:2426−2434.
18. Mintz GS, Shah VM, Weissman NJ. Regional remodeling as the cause of late stent malapposition. *Circulation* 2003;**107**:2660−2663.
19. Hassan AK, Bergheanu SC, Stijnen T, van der Hoeven BL, Snoep JD, Plevier JW, Schalij MJ, Wouter Jukema J. Late stent malapposition risk is higher after drug-eluting stent compared with bare-metal stent implantation and associates with late stent thrombosis. *Eur Heart J* 2009;**31**:1172−1180.

20. Wilson GJ, Nakazawa G, Schwartz RS, Huibregtse B, Poff B, Herbst TJ, Baim DS, Virmani R. Comparison of inflammatory response after implantation of sirolimus- and paclitaxel-eluting stents in porcine coronary arteries. *Circulation* 2009;**120**: 141–149. 141–142.

21. Nakazawa G, Finn AV, Vorpahl M, Ladich ER, Kolodgie FD, Virmani R. Coronary responses and differential mechanisms of late stent thrombosis attributed to first-generation sirolimus- and paclitaxel-eluting stents. *J Am Coll Cardiol* 2011;**57**: 390–398.

22. Otsuka F, Nakano M, Vorpahl M, Yazdani SK, Ladich E, Kolodgie F, Finn AV, Virmani R. Pathology of second- versus first-generation drug-eluting stents in humans: does safety issue still exist?. *Eur Heart J* 2011;**32**(Abstract supplement):82.

23. John MC, Wessely R, Kastrati A, Schomig A, Joner M, Uchihashi M, Crimins J, Lajoie S, Kolodgie FD, Gold HK, Virmani R, Finn AV. Differential healing responses in polymer- and nonpolymer-based sirolimus-eluting stents. *JACC Cardiovasc Interv* 2008;**1**:535–544.

24. Virmani R, Guagliumi G, Farb A, Musumeci G, Grieco N, Motta T, Mihalcsik L, Tespili M, Valsecchi O, Kolodgie FD. Localized hypersensitivity and late coronary thrombosis secondary to a sirolimus-eluting stent: should we be cautious?. *Circulation* 2004;**109**:701–705.

25. Cook S, Ladich E, Nakazawa G, Eshtehardi P, Neidhart M, Vogel R, Togni M, Wenaweser P, Billinger M, Seiler C, Gay S, Meier B, Pichler WJ, Juni P, Virmani R, Windecker S. Correlation of intravascular ultrasound findings with histopathological analysis of thrombus aspirates in patients with very late drug-eluting stent thrombosis. *Circulation* 2009;**120**:391–399.

26. Dahl OE, Westvik AB, Kierulf P, Lyberg T. Effect of monomethylmethacrylate on procoagulant activities of human monocytes and umbilical vein endothelial cells *in vitro*. *Thromb Res* 1994;**74**:377–387.

27. Risse PA, Jo T, Suarez F, Hirota N, Tolloczko B, Ferraro P, Grutter P, Martin JG. Interleukin-13 inhibits proliferation and enhances contractility of human airway smooth muscle cells without change in contractile phenotype. *Am J Physiol Lung Cell Mol Physiol* 2011;**300**:L958–L966.

28. Lanone S, Zheng T, Zhu Z, Liu W, Lee CG, Ma B, Chen Q, Homer RJ, Wang J, Rabach LA, Rabach ME, Shipley JM, Shapiro SD, Senior RM, Elias JA. Overlapping and enzyme-specific contributions of matrix metalloproteinases-9 and -12 in IL-13-induced inflammation and remodeling. *J Clin Invest* 2002;**110**:463–474.

29. Curci JA, Liao S, Huffman MD, Shapiro SD, Thompson RW. Expression and localization of macrophage elastase (matrix metalloproteinase-12) in abdominal aortic aneurysms. *J Clin Invest* 1998;**102**:1900–1910.

30. Bell MR, Garratt KN, Bresnahan JF, Edwards WD, Holmes DR Jr. Relation of deep arterial resection and coronary artery aneurysms after directional coronary atherectomy. *J Am Coll Cardiol* 1992;**20**:1474–1481.

31. Slota PA, Fischman DL, Savage MP, Rake R, Goldberg S. Frequency and outcome of development of coronary artery aneurysm after intracoronary stent placement and angioplasty. STRESS Trial Investigators. *Am J Cardiol* 1997;**79**:1104–1106.

32. Guagliumi G, Sirbu V, Musumeci G, Gerber R, Biondi-Zoccai G, Ikejima H, Ladich E, Lortkipanidze N, Matiashvili A, Valsecchi O, Virmani R, Stone GW. Examination of the *in vivo* mechanisms of late drug-eluting stent thrombosis: findings from optical coherence tomography and intravascular ultrasound imaging. *JACC Cardiovasc Interv* 2012;**5**:12–20.

33. Räber L, Magro M, Stefanini GG, Kalesan B, van Domburg RT, Onuma Y, Wenaweser P, Daemen J, Meier B, Juni P, Serruys PW, Windecker S. Very late coronary stent thrombosis of a newer-generation everolimus-eluting stent compared with early-generation drug-eluting stents: a prospective cohort study. *Circulation* 2012;**125**:1110–1121.

34. Palmerini T, Biondi-Zoccai G, Della Riva D, Stettler C, Sangiorgi D, D'Ascenzo F, Kimura T, Briguori C, Sabate M, Kim HS, De Waha A, Kedhi E, Smits PC, Kaiser C, Sardella G, Marullo A, Kirtane AJ, Leon MB, Stone GW. Stent thrombosis with drug-eluting and bare-metal stents: evidence from a comprehensive network meta-analysis. *Lancet* 2012;**379**:1393–1402.